TABLE I. Summary of Ga^{70} Data.

Calibration frequency[a] (Mc/sec)	ν Ga^{70} frequency (Mc/sec)	Electronic state	F	Magnetic field[b] (gauss)	Calculated first-order frequency ν_0 for $I=1$ (Mc/sec)	$\nu-\nu_0$ (Mc/sec)
1.510(25)	Spin=1	$^2P_{\frac{3}{2}}$	$\frac{5}{2}$	3.227(53)		
1.867(30)	4.470(100)	$^2P_{\frac{3}{2}}$	$\frac{5}{2}$	3.987(64)	4.466	+0.004
1.633(25)	1.115(100)	$^2P_{\frac{1}{2}}$	$\frac{3}{2}$	3.490(53)	1.084	+0.031
1.730(25)	5.210(125)	$^2P_{\frac{3}{2}}$	$\frac{3}{2}$	3.696(53)	5.060	+0.150
4.616(25)	11.125(90)	$^2P_{\frac{1}{2}}$	$\frac{5}{2}$	9.815(53)	10.995	+0.130

[a] Calibration in terms of the Rb^{85} (3, −2) ↔ (3, −3) transition.
[b] Calculated from the calibration frequency.

ACKNOWLEDGMENTS

We wish to thank Dr. W. B. Ewbank, Dr. F. R. Petersen, Miss B. M. Dodsworth, Mr. F. S. Baker, and Mr. J. Bowen for the help given during the critical phases of the experiment. We are also grateful to the Health Chemistry Division of the Lawrence Radiation Laboratory and the operators of the Test Reactor at Vallecitos Atomic Laboratory for their extremely rapid and careful handling of the radioactive sample. Especially, we would like to thank LCDR R. E. Roby, his crew, and the United States Navy for providing the helicopter transportation of the bombarded sample.

PHYSICAL REVIEW VOLUME 125, NUMBER 6 MARCH 15, 1962

Anomalies in Yield Curves over the 992-kev $Al^{27}(p,\gamma)Si^{28}$ Resonance*

W. L. WALTERS,† D. G. COSTELLO, J. G. SKOFRONICK, D. W. PALMER, W. E. KANE, AND R. G. HERB
University of Wisconsin, Madison, Wisconsin

(Received October 30, 1961)

Gamma-ray yields from the $Al^{27}(p,\gamma)Si^{28}$ reaction have been investigated at the 992-kev resonance using H_1^+ and H_2^+ ions on thick and thin aluminum targets. Thick-target yield curves due to proton bombardment show a prominent peak a few hundred ev above the resonance energy. This structure was predicted by Lewis and is caused by the discrete nature of the energy losses suffered by the protons as they penetrate the target. A Monte Carlo calculation gives good agreement with the general form of the experimental curve. Diatomic ion thick-target yield curves are more complex in structure than those found with protons. The largest effect here is due to Coulomb repulsion between the two protons as they pass through the target. Internal kinetic energy of the ions makes a contribution to the structure. The Lewis effect also appears to contribute. Some information regarding the relative populations of the vibrational levels of the ions was obtained from H_2^+ ion thin-target yield curves.

I. INTRODUCTION

IN previous published work, new features have been reported in thick-target gamma-ray yield curves from the $Al^{27}(p,\gamma)Si^{28}$ resonance at 992 kev. Curves taken with a proton beam of high-energy resolution have exhibited a maximum in the yield at an energy slightly above the resonance energy followed by a leveling off to a constant value at higher energies.[1] This structure was predicted by Lewis[2] and is due to the discreteness of the energy losses suffered by the protons as they penetrate the target.[3]

Dahl, Costello, and Walters[4] observed that yield curves obtained with H_2^+ ions from this resonance have a complex shape extending over a wide range of proton energies. Dahl *et al.* assumed that the binding electrons accompanying the ions are torn away immediately upon impact with the target. The ensuing Coulomb force between the protons results in large changes in the energies of the protons. Calculations based on this model succeeded in fitting thick-target yield curves taken with relatively low beam energy resolution.

In this paper results obtained with protons are

* This work was supported by the U. S. Atomic Energy Commission and by the Graduate School from funds supplied by the Wisconsin Alumni Research Foundation.

† Present address: Department of Physics, University of Wisconsin—Milwaukee, Milwaukee, Wisconsin.

[1] W. L. Walters, D. G. Costello, J. G. Skofronick, D. W. Palmer, W. E. Kane, and R. G. Herb, Phys. Rev. Letters **7**, 284 (1961).

[2] H. W. Lewis, Phys. Rev. **125**, 937 (1962).

[3] The authors have chosen to call the structure of the yield curve "the Lewis effect."

[4] P. F. Dahl, D. G. Costello, and W. L. Walters, Nuclear Phys. **21**, 106 (1960).

discussed in part II followed by a presentation of the findings with H_2^+ ions in part III.

II. RESULTS OBTAINED WITH PROTONS

A. Background

In passing through target material, charged particles lose energy in discrete steps Q due to collisions with electrons. Nuclear reactions can be produced only by those particles which spend some time between collisions near the resonance energy E_R. If particles are incident on the target at an energy well above E_R then some of them will completely jump over the resonance if the natural width of the resonance is smaller than Q_{max}, the maximum allowable energy loss in a single collision. On the other hand, if particles are incident at E_R then all of them will have for a finite time the correct energy to interact. The resulting yield curve should exhibit a peak followed by a shallow minimum and then a leveling off to the plateau height.[2]

B. Experimental Procedure

Yield curves were taken for the $Al^{27}(p,\gamma)Si^{28}$ resonance reaction at 992 kev to investigate the Lewis effect. The natural width of this resonance is[5] 80 ± 40 ev and the proton beam energy distribution had a theoretical full width at half maximum of about 300 ev. For 992-kev protons $Q_{max}=2160$ ev.

The targets used in early work were prepared by evaporating aluminum from a tungsten filament in the target chamber. Yield curves from these targets showed the Lewis effect in several instances, but without exception, after prolonged running on the target the peak in the yield flattened out and the curve assumed the conventional shape. This behavior is attributed to contamination of the surface of the target.

To reduce the problem of target contamination a new method of target preparation was developed.[6] An oven was fabricated from a molybdenum rod and used in the target chamber as shown in Fig. 1. The aluminum to be evaporated was placed inside the oven and conduction current in the molybdenum wall provided the heat for evaporation. Currents of 100 to 150 amp were required for evaporation. Commonly, 10 to 20 mg of aluminum was placed inside the oven during assembly. The heating current could be controlled so that virtually any rate of evaporation could be maintained. Target build-up rates as low as 14 A per hr were used in forming targets from 8.5 to 490 A thick.

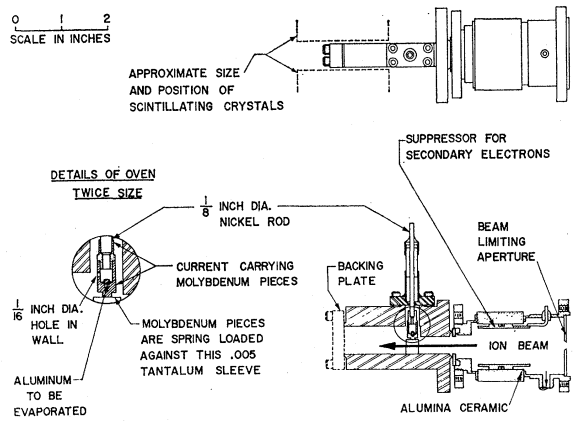

FIG. 1. Target chamber.

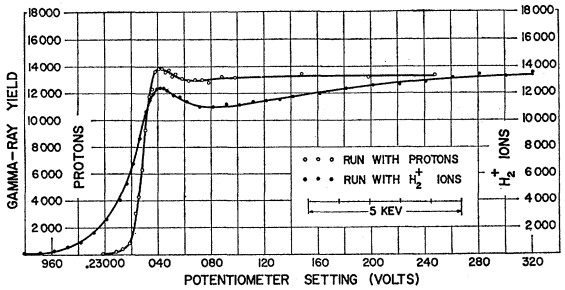

FIG. 2. Thick-target yield curves over 992-kev resonance with continuous evaporation of aluminum. Absolute energy scale is not accurately determined but proton energy is given approximately by 4.308×10^6 times potentiometer setting in volts. The H_2^+ curve has been corrected for the mass of the binding electron. Yield values given are counts per data point after subtraction of 75–100 background counts for the H_2^+ data and 400–500 background counts for the H_1^+ data.

Two detecting crystals were used in order to obtain good detector geometry. The crystals were connected to similar photomultiplier tubes and amplifiers and the counts accumulated by the two halves of the system were totaled for plotting purposes.

The ion beam was allowed to enter the target chamber during evaporation of the aluminum. After a film of sufficient thickness had condensed on the backing plate, data for thick-target yield curves were taken as evaporation continued. This procedure proved to be very advantageous. All yield curves taken during continuous evaporation exhibited a Lewis peak. The amplitudes of the peaks, however, varied by about a factor of 2. This will be discussed further in Sec. II(E).

C. Experimental Results

Thick-target yield curves taken with protons and exhibiting the Lewis effect are shown in Figs. 2 and 3. The companion curves in the figures are thick target yield curves taken with H_2^+ ions which are discussed in Part III. Data for the curves in both Figs. 2 and 3 were taken during continuous evaporation of aluminum. In Fig. 3 the yield curve from protons was taken prior to the run with H_2^+ ions and the yield curves show the effects of increased target thickness.

Figure 4 shows data taken from a target prepared by evaporation from a filament. Run A, which is only partially shown in Fig. 4, was taken with protons on the

[5] Jerry B. Marion, Revs. Modern Phys. **33**, 139 (1961).
[6] W. L. Walters, Ph.D. thesis, University of Wisconsin, Madison, Wisconsin, 1961 (unpublished).

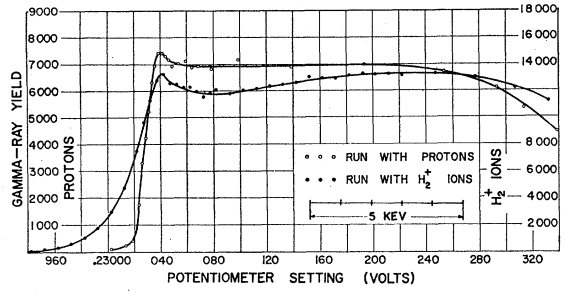

FIG. 3. Thick-target yield curves over 992-kev resonance with continuous evaporation of aluminum. Target not yet sufficiently thick to show full structure of H_2^+ curve. Absolute energy scale is not accurately determined but proton energy is given approximately by 4.308×10^6 times potentiometer setting in volts. The H_2^+ curve has been corrected for the mass of the binding electron. Yield values given are counts per data point after subtraction of 250–300 background counts for the H_2^+ data and 350–450 background counts for the H_1^+ data.

freshly evaporated target and it exhibits the Lewis effect. Runs B and C were with H_2^+ ions. They were followed by run D with protons. The mid-points and interquartile widths[7] of both yield curves A and D are the same, yet one shows the Lewis effect and the other does not. It is believed that the disappearance of the peak is due to the slow accumulation of surface contaminants on the target.

D. Interpretation

The probability per unit path length $p(Q,E)dQ$ that a charged particle of energy E will suffer an inelastic collision with an electron in which an amount of energy between Q and $Q+dQ$ is lost is given approximately by

$$p(Q,E)dQ=(K/EQ^2)dQ, \tag{1}$$

where K can be considered a constant for heavy nonrelativistic particles.[8] The $1/Q^2$ dependence is used for most purposes although it is known that the probability function has large resonance peaks for values of Q near atomic excitation energies.

Any value of Q between certain limiting values is permissible. The maximum energy loss Q_{max} is taken as the energy loss in a head-on collision of an incident particle with a free electron. The minimum energy loss, Q_{min}, is assumed by Block to be given by[9]

$$Q_{min}=I^2/Q_{max}, \tag{2}$$

where I is the mean ionization energy of the stopping material. The value of I is experimentally determined by fitting the gross stopping power of the target material.

As a monoenergetic beam of particles at energy E_i penetrates the target, particles are removed from the energy group E_i when they suffer their first collision.

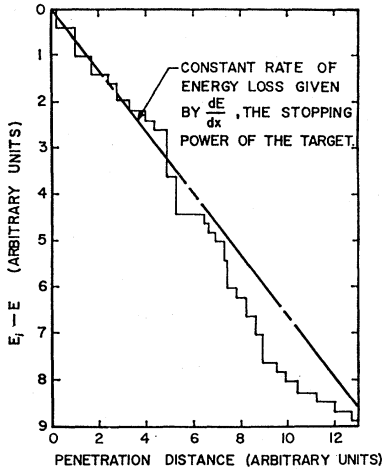

FIG. 5. Schematic diagram showing the energy losses suffered by a proton as it penetrates a target. Proton energy E is plotted relative to the incident energy E_i.

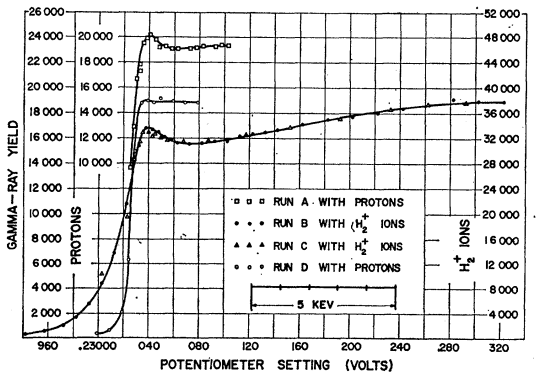

FIG. 4. Thick-target yield curves over 992-kev resonance. Aluminum target was prepared before taking data by evaporation from a tungsten filament. Effects of contaminant build up are observed.

If N particles pass through the target, the number which suffer a collision in a distance dx is

$$dN=-N\lambda dx, \tag{3}$$

where λ is a constant. This expression shows that the incident beam decays exponentially from energy E_i into the lower energy region as it penetrates the target.

The value of λ in Eq. (3) can be considered a constant of the stopping material for all particles with energy E not greatly different from E_i. Particles will therefore travel the mean distance $\bar{X}=1/\lambda$ between the first and second collisions, the same distance $\bar{X}$ between the second and third collisions, and so forth.

The yield per proton at a mean beam energy E_b

[7] The interquartile width is the energy increase required for the yield curve to increase from $\frac{1}{4}$ to $\frac{3}{4}$ of the total height.

[8] R. D. Evans, *The Atomic Nucleus* (McGraw-Hill Book Company, Inc., New York, 1955), Chaps. 18, 22.

[9] F. Bloch, Z. Physik **81**, 363 (1933).

from an infinitely thick homogeneous target is given by[10]

$$Y(E_b)=n_A\int_{x=0}^{\infty}\int_{E_i=0}^{\infty}\int_{E=0}^{\infty} g(E_b,E_i)W(x,E,E_i)\times\sigma(E_R,E)dEdE_idx, \quad (4)$$

where n_A is the number of aluminum atoms per unit volume, $g(E_b,E_i)dE_i$ is the probability that a proton in a beam of mean energy E_b has an incident energy between E_i and E_i+dE_i, $W(x,E,E_i)dE$ is the probability that a proton incident on the target at an energy E_i has an energy between E and $E+dE$ at a depth x into the target, and $\sigma(E_R,E)$ is the cross section for the resonance.

A function η is now defined such that

$$\eta(E_i-E)dE=\left[\int_{x=0}^{\infty} W(x,E,E_i)dx\right]dE, \quad (5)$$

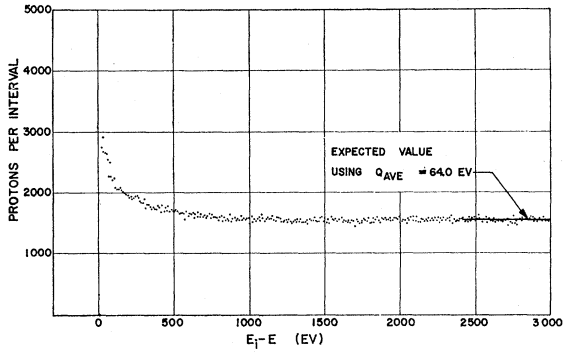

FIG. 6. Results of Monte Carlo calculations for 10 000 incident protons. The energy region below the incident energy E_i was divided into 10-ev intervals. Data points show how many protons entered each energy interval. All 10 000 were put into the 0–10 ev interval. This point is not shown on the curve.

represents the probability that a proton incident at an energy E_i has an energy between E and $E+dE$ somewhere inside the target. With this expression Eq. (4) becomes

$$Y(E_b)=n_A\int_{E_i=0}^{\infty}\int_{E=0}^{\infty} g(E_b,E_i)\sigma(E_R,E)\times\eta(E_i-E)dEdE_i, \quad (6)$$

where $\eta(E_i-E)=0$ for $E>E_i$. Thus, if the resonance cross section is approximated by a delta function $\delta(E_R-E)$, the function $\eta(E_i-E)$ gives the yield per proton, at energy E_i, from a monoenergetic beam for which $g(E_b,E_i)=\delta(E_b-E_i)$.

Figure 5 schematically traces the energy losses of a single proton, incident on the target at an energy E_i, as it penetrates the target. The over-all slope of the path in Fig. 5 is given by the gross stopping power dE/dx of aluminum. The energy losses Q take place in discrete steps of sizes limited by $Q_{\min}\leq Q\leq Q_{\max}$. Between collisions the particle remains at a constant energy and if its energy is correct it may undergo radiative capture. Many particles enter the target at E_i and each traces out such a stepwise pattern as it penetrates the target, although details of the pattern will be different for each particle.

The distribution in sizes of the vertical jumps Q in Fig. 5 is governed by the $1/Q^2$ law of Eq. (1). A computer was programmed to pick random numbers m with equal probability from the open interval (0,1). These numbers were used to determine values of Q distributed according to the $1/Q^2$ relationship between $Q_{\max}$ and $Q_{\min}$. Each value of Q found in this manner was subtracted from the energy of the particle.

In the program the region below the incident energy E_i is divided into adjoining intervals $(\Delta E)_j$ each 10 ev wide. The program chooses a value of Q and subtracts it from the energy E_i. The computer then determines in which interval $(\Delta E)_j$ the resultant energy E lies. After this a second value of Q is subtracted from E and a new determination of the interval $(\Delta E)_j$ is made. The computer repeats this process until $(E_i-E)\geq 3$ kev at which time the entire process is repeated on a second proton with an initial energy E_i. Many particles are allowed to cascade downward through the intervals $(\Delta E)_j$ and the computer keeps a running total of how many stops A_j are made in each interval $(\Delta E)_j$. The histogram made by plotting A_j vs the mean energy of the jth interval is a good approximation to the function $\eta(E_i-E)$ if the total number of particles processed by the program is large and if the accumulated numbers A_j are not too small.

For 992-kev protons $Q_{\max}=2160$ ev and, using a recently measured value of $I=163$ ev,[11] Eq. (2) gives $Q_{\min}=12.3$ ev. A total of 10 000 protons were allowed to drop in energy, one at a time, until $(E_i-E)\geq 3$ kev. The histogram of the computer results using these parameters is shown in Fig. 6. This figure shows how many protons spend time in each energy interval if 10 000 protons are incident at energy E_i. The average time spent per proton is the same for all energy intervals.

The horizontal line at 3 kev below E_i represents the number of protons expected per energy interval deep in the target where the average energy loss $Q_{\text{av}}=64.0$ ev. For 10 000 incident particles, 1563 particles appear in each interval. The histogram values near $E=E_i$ have also been checked with quantitative calculations and agreement is good.

Several thin-target yield curves were taken over the 992-kev resonance in aluminum. The data obtained from a target of 60-ev thickness[12] are shown in Fig. 7. The asymmetry shown by the experimental data is

[10] H. E. Gove, in *Nuclear Reactions*, edited by P. M. Endt and M. Demeur (North-Holland Publishing Company, Amsterdam, 1959), Vol. I, p. 293.

[11] H. Bichsel and E. A. Uehling, Phys. Rev. **119**, 1670 (1960).

[12] Target thicknesses are given in terms of the average energy loss for 1-Mev protons.

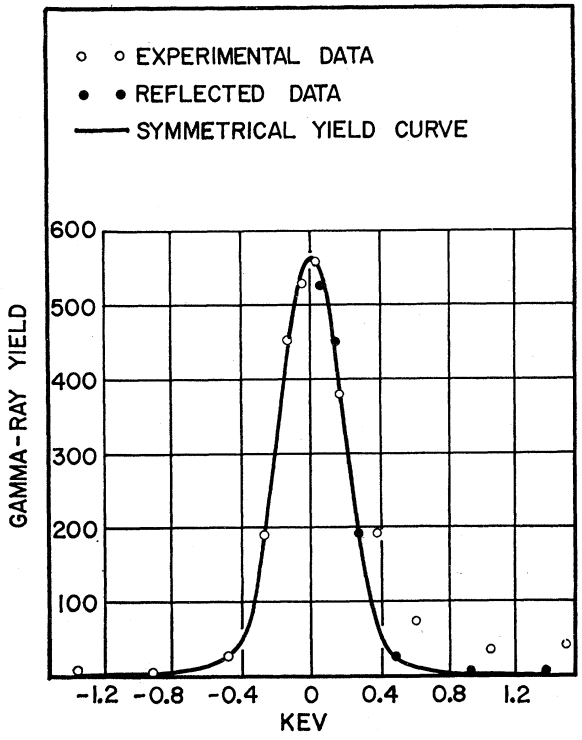

FIG. 7. Symmetric yield curve for H_1^+ ions on aluminum target[12] 60 ev thick. High-energy half of the curve was formed by reflection of the low-energy half through the peak.

partially due to straggling and may be partially due to nonuniformities in the target thickness. A symmetric curve was formed by reflecting data points from the low-energy side of the curve across the peak to form the high-energy portion of the curve. The resulting curve was assumed to represent the total effect on the yield of beam energy spread, Doppler broadening, and resonance width. Products of these thin-target yield values and the $\eta(E_i-E)$ values were integrated graphically. For computational purposes it was assumed that E_b and E_R coincide at the peak of the symmetric thin-target yield curve. The calculated yield curve is compared in Fig. 8 with the experimental data giving the highest Lewis peak observed. These data were taken during continuous evaporation.

E. Discussion

The calculated yield curve indicates a shift in the point normally considered to be the resonance energy E_R. On experimental thick-target yield curves E_R has conventionally been taken as the position of half maximum yield. The calculated curve in Fig. 8 indicates that for the present experimental conditions the half-value point on the yield curve falls at an energy about 100 ev below E_R.

The Lewis peak in the experimental data does not rise as high as that on the calculated curve. Several factors are believed to contribute to this difference. The amplitudes of the Lewis peaks on experimental curves vary by about a factor of two. This suggests that variations in the targets are influencing the yield curves. With the continuous evaporation procedure some volume impurities are to be expected. It is believed improbable, however, that differences in volume impurities contribute greatly to the variations between experimental curves. These differences are probably due principally to variations in surface contaminants still present with continuous evaporation.

Some of the difference between the calculated yield curve and the data of Fig. 8 is probably due also to surface contaminants. An experimental curve from a pure aluminum target with no surface film would probably have a peak height appreciably higher than that displayed by the data in Fig. 8. On the other hand, the peak in the calculated curve may be too high because of approximations in stopping power formulas.

To establish the relationship between the size of the Lewis peak and the value of $Q_{\min}$ and $Q_{\max}$ the computer program was run several times with values of $Q_{\min}=6.15$, 12.3, and 24.6 ev and values of $Q_{\max}=2160$ and 4320 ev. It was found that the area under the peak increases as either $Q_{\min}$ or $Q_{\max}$ is increased.

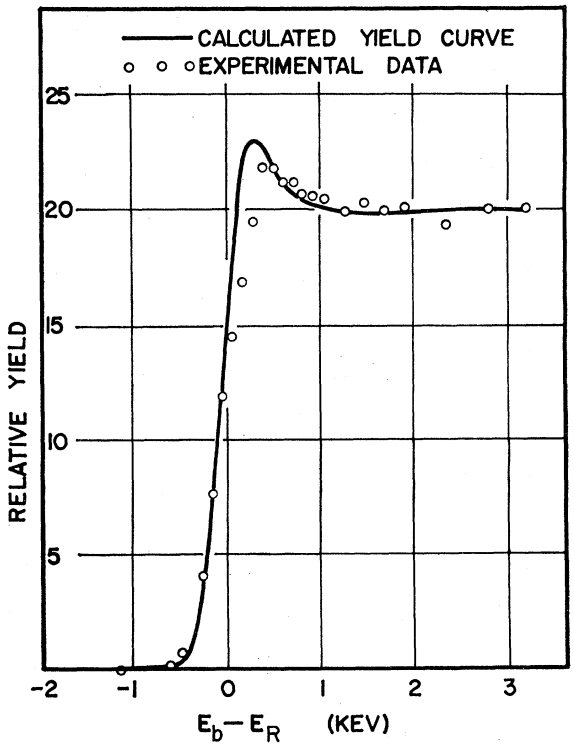

FIG. 8. Comparison of calculated yield curve with experimental data showing the highest observed Lewis peak. Yield values are fitted in upper energy region and energy values are fitted at half plateau height. Mean beam energy E_b is plotted relative to resonance energy E_R.

F. Conclusion

The presence of the Lewis effect has been established for the 992-kev resonance in aluminum. Targets relatively free of surface contaminants are required to show it consistently. Calculations based on stopping power theory indicate that the resonance energy does not coincide with the point of half maximum yield on a thick-target yield curve.

III. RESULTS WITH H_2^+ IONS

A. Background

Previous workers have taken yield curves from resonances in pairs, one curve with the proton beam and a second curve with the H_2^+ ion beam at twice the energy. Several differences in the shapes of the yield curves have been noted.

Herring, Douglas, Silverstein, and Chiba found that thin-target yield curves taken with H_2^+ ions were broader than those taken with the proton beam.[13] On thick-target yield curves taken at Oslo, Andersen, Gjötterud, Holtebekk, and Lönsjö found that the interquartile widths[7] of curves taken with H_2^+ ions were considerably greater than those taken with protons.[14] The Oslo group also noted that measurements of the resonance energy E_R from diatomic-ion curves led to lower values than similar measurements from yield curves taken with the proton beam. The observed broadening in both thick- and thin-target curves was attributed to the internal motion of the protons within the H_2^+ ions. One ev per proton of internal energy can account for a ± 2-kev spread in the laboratory energy of 1-Mev protons in an H_2^+ ion beam. Andersen *et al.*, attributed the shift between thick-target yield curves to nonlinearity in the electrostatic analyzer used in the experiment.

Subsequent work by Bondelid and Kennedy showed that the energy shift was not experimental in origin.[15] Bondelid and Kennedy ran both thick- and thin-target yield curves and, whereas thick-target curves showed the shift in energy, there was no unexplainable shift between thin-target curves. Bondelid and Kennedy also noted that the leading edge of thick-target yield curves taken with H_2^+ ions had a curious asymmetry.

Dahl, Costello, and Walters studied the problem further[4] and showed that previously published thick-target yield curves from H_2^+ ion bombardment were incomplete. To fully record the yield from the resonance in aluminum at 992 kev, for instance, data must be taken until the proton energy is about 10 kev above the resonance energy.

To account for their diatomic-ion yield curves Dahl, Costello, and Walters assumed that the molecular ion loses its binding electron immediately when it strikes the target. In the absence of the binding electron the repulsive Coulomb force between the protons makes itself felt. The impulses received by the protons depends upon their initial separation and may have a large effect on the laboratory energy of the protons. In particular, for an ion which breaks up with its internuclear axis aligned with the beam direction, the front proton, near the surface of the target, may receive energy from the Coulomb field at a rate greater than the normal ionization energy loss.[6,16] Thus, the forward proton may pass through the resonance energy twice.

Using this model Dahl, Costello, and Walters calculated a yield curve for a monoenergetic incident beam of H_2^+ ions with no internal kinetic energy. The initial separation of the protons was considered to be their equilibrium separation of 1.06 A. Effects of the internal kinetic energies of the ions were lumped into the beam energy distribution.

The shape of calculated curves led Dahl, Costello, and Walters to predict that H_2^+ ion yield curves taken with higher energy resolution should have a broad peak due to Coulomb effects at energies just above the resonance energy. The present work was undertaken with higher energy resolution and with better quality targets in an effort to observe this peak and to establish more precisely the energy shift between thick-target H_1^+ and H_2^+ ion curves. An attempt was also made to determine the mean internal energy of the ions.

B. Experimental Procedure and Form of Thick-Target Curves

Experimental work was confined to the gamma-ray resonance in aluminum at 992 kev. The work reported here was done with the same energy resolution and targets as the proton work of part II. Yield curves were generally taken in pairs, one with protons and one with diatomic ions.

Figures 2 and 3 show data taken during continuous evaporation. The H_2^+ ion yield curves show the peak predicted by Dahl, Costello, and Walters. Figure 3 indicates that the target was of insufficient thickness to allow complete Coulomb separation of the protons. Figure 2 is a complete pair of thick-target yield curves.

As with the proton work the effects of target contamination could be seen on yield curves taken with H_2^+ ions. Figure 4 illustrates this. The data from run *B* were taken several hours before the data from run *C*. With accumulation of contamination the height of the peak in the yield curve diminished. This effect was observed several times with targets prepared by evaporation from a filament. In runs taken during continuous evaporation however, no such effect was seen.

[13] D. F. Herring, R. A. Douglas, E. A. Silverstein, and R. Chiba, Phys. Rev. **100**, 1239 (1955).
[14] S. L. Andersen, K. Gjötterud, T. Holtebekk, and O. Lönsjö, Nuclear Phys. **7**, 384 (1958).
[15] R. O. Bondelid and C. A. Kennedy, Naval Research Laboratory Report NRL-5083 Washington, D. C., 1958 (unpublished).
[16] P. F. Dahl, Ph.D. thesis, University of Wisconsin, Madison, Wisconsin, 1960 (unpublished).

TABLE I. Energy shifts observed between H_1^+ and H_2^+ thick-target curves.

Resonance run No.	Approx. target thickness (kev)[b]	Method of preparation[c]	Energy shift (ev)
Results of Dahl, Costello, and Walters[a]			
L	≈50	Foil	640[e]
M	≈50	Foil[d]	730
N	≈50	Foil[d]	570
Present results			
X	>15	Fil. evaporation	330
Y	≈10	Oven evaporation	280[e]
Z	≈23	Oven evaporation	300

[a] See reference 4.
[b] See reference 12.
[c] For a description of the foil targets see reference 4.
[d] The two pairs of runs, *M* and *N*, were made on the same foil target.
[e] Data for the yield curve from diatomic ions were not taken at beam energies high enough to reveal the final leveling off of the curve. The height of the proton curve was used for a maximum yield value in these cases.

C. Energy Shift

The energy shift between proton yield curves and H_2^+ ion yield curves was measured on several pairs of thick-target curves. The measurements were made between the points of half the plateau yield on the curves. Table I shows the energy shifts found from several pairs of curves. The measurements were made after the H_2^+ ion yield curve was corrected for the mass of the binding electron. In all cases the midpoint of the yield curve taken with protons came at the higher energy. The original data of Dahl, Costello, and Walters were used for the entries indicated. It appears that the energy shift depends on the energy resolution and perhaps on contaminants. Further work is needed before thick-target yield curves with H_2^+ ions can be used for energy calibrations.

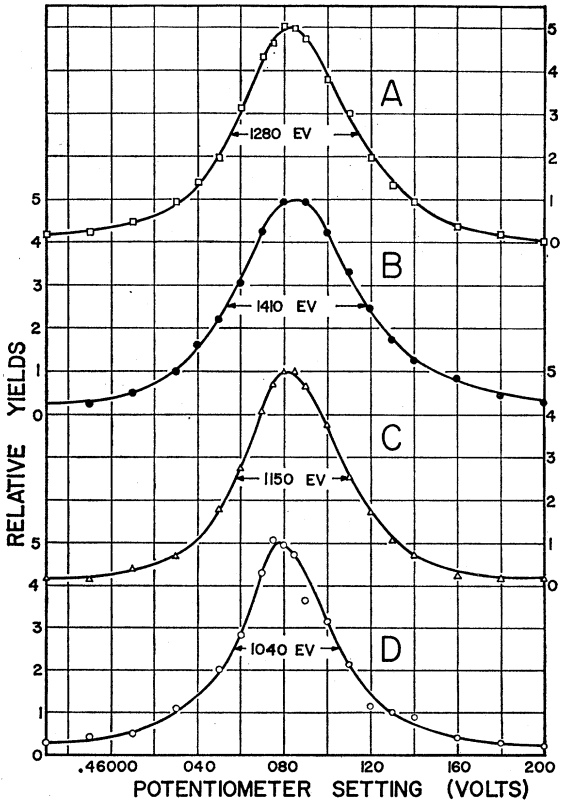

FIG. 9. Yield curves for H_2^+ ions from thin aluminum targets. Target thicknesses[12] are: curve *A*, 350 ev; curve *B*, 260 ev; curve *C*, 150 ev; curve *D*, 40 ev. Yield values are normalized for equal peak heights.

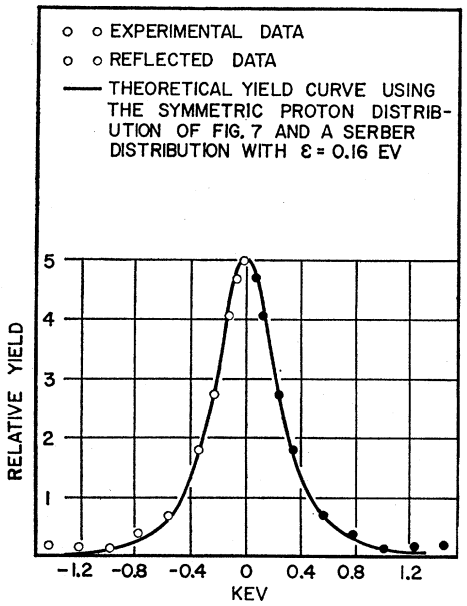

FIG. 10. Fit to the data taken with H_2^+ ions from the 150-ev target of Fig. 9. Data have been made symmetric in this figure.

D. Thin Targets

1. *Experimental Curves*

Figure 9 shows several thin-target curves taken with diatomic ions. The yields have been normalized so that peak heights of all four curves are the same. The targets were evaporated from the oven of Fig. 1 and their thicknesses[12] were determined by dividing the area beneath the thin-target curves by the maximum yield obtained from a thick-target taken with the same geometry.[17]

The curves show no simple relationship between target thicknesses and widths. The yield curve from the 260-ev target, for example, is broader than that from the 350-ev target. Such diversities have been noticed on other thin-target curves taken with diatomic ions. Variations such as these could be caused by contaminating films on the aluminum, by target lumpiness, or they might indicate that the mean vibrational energy of the ions depends on the ion source

[17] E. J. Bernet, R. G. Herb, and D. B. Parkinson, Phys. Rev. 54, 398 (1938).

conditions or vacuum conditions along the beam path [see Sec. III (D.3) below]. An attempt was made to study the widths of H_2^+ ion thin-target yield curves as a function of ion source conditions, but the results were inconclusive.

2. *Internal Kinetic Energies—Experimental*

Following the procedure of Dahl *et al.* the thin-target yield curves taken with H_2^+ ions were fitted using the Serber formula[18]

$$n(E_m,E)=\frac{\mathcal{E}E_m}{[(E-\frac{1}{2}E_m)^2+\mathcal{E}E_m]^{\frac{1}{2}}}, \qquad (7)$$

where E_m is the energy of a monoenergetic beam of H_2^+ ions, $\mathcal{E}$ is the mean internal kinetic energy of the H_2^+ ions, and E is the laboratory energy of a proton.

The symmetric thin-target yield curve of Fig. 7 was assumed to represent the broadening introduced in the yield curve due to finite beam energy resolution, Doppler broadening, and resonance width. Products of values of the curve of Fig. 7 and values of several Serber distributions were integrated for comparison with experimental curves. In Fig. 10 one of the calculated curves is compared with the thin-target data from the 150-ev target. The Serber distribution used to obtain the curve shown in Fig. 10 had a value of $\mathcal{E}=0.16$ ev. The data from the 260- and 350-ev target were fitted successfully using Serber distributions with $\mathcal{E}=0.27$ ev (and $\mathcal{E}=0.21$ ev), respectively.[6]

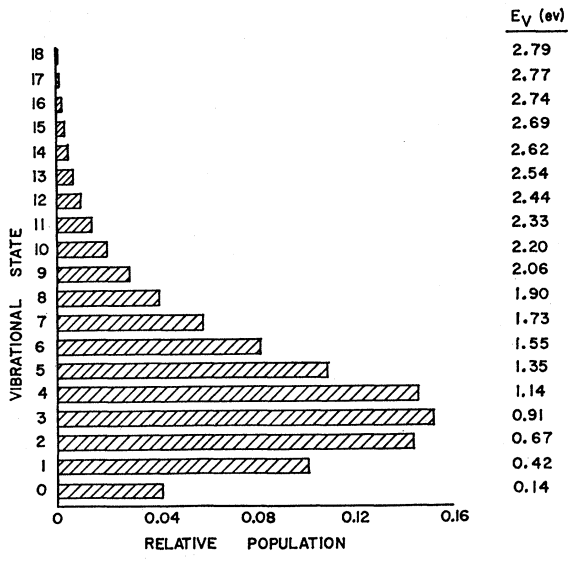

FIG. 11. Populations of the vibrational states of H_2^+ ions calculated using the Franck-Condon principle. Values of E_v give the position of the energy eigenvalues above the minimum in the H_2^+ ion potential. [E. A. Hylleraas, Z. Physik **71**, 739 (1931); S. Cohen, J. R. Hiskes, and R. J. Riddell, Jr., Phys. Rev. **119**, 1025 (1960).]

[18] R. Serber, Phys. Rev. **72**, 1008 (1947).

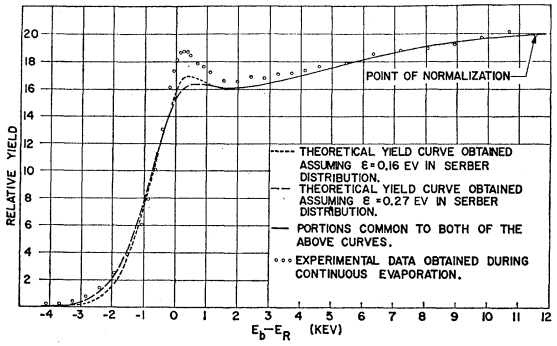

FIG. 12. Comparison of theoretical thick-target yield curves with experimental data. Yield values are fitted at the point shown. Mean beam energy, E_b, is plotted relative to the resonance energy, E_R.

3. *Internal Kinetic Energies—Calculated*

The shapes of the H_2^+ ion and H_2 molecular potentials are sufficiently different so that in the ionization process H_2^+ ions are formed in excited vibrational states. The relative populations of the vibrational states can be calculated from the Franck-Condon principle.[19] These calculations were done graphically using previously tabulated vibrational state wave functions for the H_2^+ ion[20] and using the ground-state wave function for a harmonic oscillator as an approximation to the ground-state wave function for the H_2 molecule.[21] Results are shown in Fig. 11.[22]

Since the H_2^+ ion is homonuclear de-excitation of the vibrational states by dipole radiation transitions is ruled out. Only relatively improbable quadrupole emission is allowed. Hence, the ions delivered to the target should have essentially the same distribution in vibrational states with which they are formed. A rough estimate of the mean internal kinetic energy to be expected from the distribution of Fig. 11 gave a value of 0.5 ev. On the other hand, the fit to the thin-target data gave values from 0.16 to 0.27 ev.

The reason for this discrepancy is not clear. It is possible, as Hiskes has suggested,[23] that the cross section for dissociation of the ions is highly dependent on the vibrational levels and those ions which are highly excited may be removed from the beam on their way to the target by collisions with gas molecules in the accelerating tube and vacuum system.

[19] See, for instance G. Herzberg, *Molecular Spectra and Molecular Structure* (D. Van Nostrand Company, Inc., Princeton, New Jersey, 1950), p. 193ff.

[20] S. Cohen, J. R. Hiskes, and R. J. Riddell, Jr., University of California Radiation Laboratory Report UCRL-8871, 1959 (unpublished).

[21] For any reasonable ion-source gas temperature, only the ground state of the H_2 molecule need be considered. See p. 123 of reference 19.

[22] The results obtained graphically at this laboratory agree well with results obtained independently by J. R. Hiskes using a computer.[23] The authors are indebted to Dr. Hiskes for supplying his results for comparison.

[23] J. R. Hiskes (private communications, 1961).

E. Fit to Thick-Target Curves

An attempt was made to fit the thick-target yield curves obtained with diatomic ions. The thin-target curves calculated with $\mathcal{E}=0.16$ and 0.27 ev were used as approximations to the proton energy distribution in the H_2^+ ion beam. The thick-target yield curve for a monoenergetic beam of H_2^+ ions (the same curve originally used by Dahl, Costello, and Walters) was integrated with these distributions. The calculated yield curves are compared in Fig. 12 with data taken during continuous evaporation of aluminum. The calculated yield curves do not rise high enough near the resonance energy. The use of a still smaller value of $\mathcal{E}$ adds to the calculated yield in this region but with such a distribution the fit to the data is worse on the toe of the curve, where the mean beam energy is 1 to 4 kev below the resonance energy.

Some of the difference between the calculated curves and the data is believed to be due to the Lewis effect. Protons from H_2^+ ions in which the internuclear axis is near 90° with respect to the beam direction receive practically no change in laboratory energy due to Coulomb repulsion. Their energy spread is close to that of protons in the H_1^+ beam and hence they may give additional yield at the Lewis peak. The same calculated curves were compared with data taken from a target which was known to be sufficiently contaminated so that the Lewis effect did not appear on a companion curve taken with protons. The agreement was better than on Fig. 12 but still not excellent.

The disagreement may be partially due to the assumption in the calculations that all protons begin separating from the same internuclear separation. Even though the thin-target curves indicate that the mean vibrational energy of the ions is small, there is motion of the protons within the ions and a range of initial internuclear separations should probably be taken into account.

F. Conclusion

The general form of thick-target yield curves predicted by Dahl, Costello, and Walters has been verified, but accurate theoretical fits to the data cannot be expected until the Lewis effect, the Coulomb energies, and vibrational kinetic energies of the H_2^+ ions are accurately taken into account. Thin-target work with H_2^+ ions indicates that the mean vibrational kinetic energy of the ions striking the targets is appreciably lower than that of newly formed ions.

ACKNOWLEDGMENTS

The authors acknowledge the many helpful discussions with Professor M. E. Ebel, Professor H. W. Lewis, Professor R. G. Sachs, and Professor K. R. Symon. The authors also wish to thank John Albright for his help in programming the computer and Dr. John R. Hiskes for supplying his results for the Franck-Condon calculations and for his other helpful suggestions.